Predicting Tinnitus Pitch from Patients' Audiograms with a Computational Model for the Development of Neuronal Hyperactivity

Roland Schaette[1,2,3,*] and Richard Kempter[1,2,3,4]

Affiliations:
[1] Institute for Theoretical Biology
Department of Biology
Humboldt-Universität zu Berlin
Invalidenstr. 43
10115 Berlin, Germany

[2] Bernstein Center for Computational Neuroscience Berlin
Philippstr. 13
10115 Berlin, Germany

[3] Neuroscience Research Center
Charité, Medical Faculty of Berlin
Charitéplatz 1
10117 Berlin, Germany

[4] NeuroCure Center for Neurosciences Berlin

[*] Current address: UCL Ear Institute

text pages: 24
figures: 5
Keywords: Tinnitus, hearing loss, neuronal hyperactivity, homeostatic plasticity, computational model, auditory system

Correspondence: Roland Schaette
UCL Ear Institute
University College London
332 Gray's Inn Rd
London WC1X 8EE
Tel: (44) 20 7679 8946
Fax: (44) 20 7679 8990
email: r.schaette(at)ucl.ac.uk

Abstract

Tinnitus is often related to hearing loss, but how hearing loss could lead to tinnitus has remained unclear. Animal studies show that the occurrence of tinnitus is correlated to increased spontaneous firing rates of central auditory neurons, but mechanisms that give rise to such hyperactivity have not been identified yet. Here we present a computational model that reproduces tinnitus-related hyperactivity and predicts tinnitus pitch from the audiograms of tinnitus patients with noise-induced hearing loss and tone-like tinnitus. Our key assumption is that the mean firing rates of central auditory neurons are controlled by homeostatic plasticity. Decreased auditory nerve activity after hearing loss is then counteracted through an increase of the neuronal response gain, which restores the mean rate but can also lead to hyperactivity. Hyperactivity patterns calculated from patients' audiograms exhibit distinct peaks at frequencies close to the perceived tinnitus pitch, corroborating hyperactivity through homeostatic plasticity as a mechanism for the development of tinnitus after hearing loss. The model suggests that such hyperactivity, and thus also tinnitus caused by cochlear damage, could be alleviated through additional stimulation.

Introduction

Tinnitus is the perception of a phantom sound in the absence of a corresponding acoustic stimulus. In many cases, tinnitus is related to hearing loss: The majority of tinnitus patients are affected by hearing loss (Nicolas-Puel et al., 2002), the hearing thresholds of tinnitus subjects are elevated compared to age-matched controls (Roberts et al., 2008), and the occurrence of tinnitus is related to steep audiogram slopes (König et al., 2006). Interestingly, the perceived pitch of the tinnitus sensation corresponds to frequencies where hearing is impaired (Henry et al., 1999; Noreña et al., 2002; König et al., 2006). Moreover, tinnitus patients with normal audiograms show evidence of limited cochlear damage (Shiomi et al., 1997; Weisz et al., 2006). On the other hand, there are also forms of tinnitus that are not linked to hearing loss, like for example pulsatile tinnitus or somatic tinnitus (Møller, 2007).

In animals, hearing loss through acoustic trauma can lead to increased spontaneous firing rates (Kaltenbach and McCaslin, 1996; Brozoski et al., 2002; Noreña and Eggermont, 2003; Ma et al., 2006) and increased synchronization of the spontaneous neuronal discharge (Noreña and Eggermont, 2003) of central auditory neurons. The earliest stage where increased spontaneous firing rates were found was the dorsal cochlear nucleus (DCN, Kaltenbach and McCaslin, 1996), and the degree to which the spontaneous firing rates were elevated was correlated to the strength of behavioral evidence for tinnitus (Kaltenbach et al., 2004). However, how cochlear damage could lead to such hyperactivity, and which plasticity mechanisms are involved, has remained unclear.

How hearing loss could give rise to tinnitus-related activity patterns in central auditory neurons has been the focus of theoretical modeling studies. In the "auditory brainstem model" (Gerken, 1996), lateral inhibition is assumed to exaggerate discontinuities in the spontaneous or driven output of the cochlea across frequencies, like for example a drop in spontaneous firing rates created by hearing loss. The resulting peak-like activity patterns are proposed as a basis for a tinnitus sensation (Gerken, 1996). Recent modeling studies have addressed the issue of how an increased response gain of central auditory neurons after hearing loss elevates spontaneous firing rates (Schaette and Kempter, 2006; Dominguez et al., 2006; Parra and Pearlmutter, 2007) and enhances neuronal synchrony (Dominguez et al., 2006), as observed in animal models of tinnitus. We have proposed that a stabilization of the mean firing rates of central auditory neurons through homeostatic plasticity after hearing loss could be the underlying mechanism for such an increase in response gain (Schaette and Kempter, 2006, 2008). Homeostatic plasticity is a mechanism that changes neuronal activity on time scales of hours to days by scaling synaptic strengths and regulating neuronal excitability (Turrigiano, 1999).

So far, computational models of tinnitus based on homeostatic plasticity (Schaette and Kempter, 2006) or gain adaptation and lateral inhibition (Parra and Pearlmutter, 2007) have

reproduced the relation between tinnitus pitch and hearing loss in a qualitative way only. In this study, we go one step further and perform a quantitative comparison between model predictions of tinnitus pitch and patient data. Therefor we combine a computational tinnitus model based on homeostatic plasticity (Schaette and Kempter, 2006, 2008) and lateral inhibition (Gerken, 1996) in one framework. We then apply this framework to data from tinnitus patients with noise-induced hearing loss and tone-like tinnitus (König et al., 2006) and estimate a tinnitus pitch from the audiograms of the patients. We find that neuronal hyperactivity through homeostatic plasticity is essential for obtaining model predictions of tinnitus pitch that are consistent with patient data.

Methods

Patient Data: Audiograms and Tinnitus Pitch

Our sample of tinnitus patients consists of 24 male subjects with work-related noise-induced hearing loss and tone-like tinnitus in both ears. This sample constitutes the subgroup of all patients with tone-like tinnitus but excludes the 17 patients with noise-like tinnitus and the 30 patients with no tinnitus of the data analyzed in a previous study (König et al., 2006). Pure-tone audiometry was performed with a clinical audiometer using 10 different frequencies (0.125, 0.25, 0.5, 1, 1.5, 2, 3, 4, 6, and 8 kHz). Tinnitus pitch was determined by equating the pitch of a pure tone (0.125, 0.25, 0.5, 1, 1.5, 2, 3, 4, 6 and 8 kHz) to the most prominent tinnitus pitch (see König et al., 2006, for details).

We used the edges of audiograms as a simple reference model for tinnitus pitch prediction. Audiogram edges were detected in a two-step process: First we determined the frequency range where hearing levels had not dropped more than 20 dB below the best hearing level observed in the audiogram. In this range, we looked for a local maximum of the second derivative of the audiogram to identify the audiogram edge. If no edge could be identified in that way, the highest frequency that still met the 20 dB hearing level criterion was said to be the audiogram edge.

Computational Model

To test hypotheses of how hearing loss can lead to tinnitus, we set up a simple phenomenological model of several processing stages of the auditory pathway: the auditory nerve (AN), the dorsal cochlear nucleus (DCN), and a layer with lateral inhibition as found in higher stages of the auditory pathway like, for example, the inferior colliculus and/or the auditory cortex (Fig. 1a). The model is phrased in terms of average firing rates of small populations of neurons, i.e., all model neurons represent populations of real neurons. The model is organized in frequency channels that are arranged tonotopically from low to high frequencies, with 10 frequency channels per octave. Below we briefly describe the main properties of the computational model. Details can be found in Schaette and Kempter (2006, 2008).

Acoustic Environment, Auditory Nerve Model, and Hearing Loss

We assume that the probability density function $p_{\mathrm{I}}(I)$ of the sound intensity levels I (in units of dB) encountered in a typical acoustic environment can be approximated by a Gaussian dis-

tribution with a mean intensity of $\mu_I = 40\,\mathrm{dB}$ and a standard deviation of $\sigma_I = 25\,\mathrm{dB}$:

$$p_I(I) = \frac{1}{\sqrt{2\pi\sigma_I^2}} \exp\left(-\frac{(I-\mu_I)^2}{2\sigma_I^2}\right) \tag{1}$$

We assume the same intensity distribution for all frequency channels (Fig. 1a).

Each frequency channel in our AN model comprises a small population of AN fibers with similar characteristic frequencies but different response thresholds and different spontaneous firing rates. The activity of the AN fiber population in each frequency channel is described by a population firing rate $f(I)$:

$$f(I) = \begin{cases} f_{sp} & \text{for} \quad I < I_{th}, \\ f_{sp} + (f_{max} - f_{sp}) \dfrac{\int_{I_{th}}^{I} \mathrm{d}I'\, p_I(I')}{1 - P_{sp}} & \text{for} \quad I \geq I_{th}. \end{cases} \tag{2}$$

The probability of occurrence of spontaneous activity is $P_{sp} = \int_{-\infty}^{I_{th}} \mathrm{d}I\; p_I(I)$; a value of $P_{sp} = 0.05$, for example, means that 5% of the time the AN fibers are active at the spontaneous firing rate f_{sp}. By definition, the response threshold of the healthy AN fiber population is $I_{th} = 0\,\mathrm{dB}$ hearing level (dB HL). For sub-threshold stimuli, there is spontaneous activity at $f_{sp} = 50\,\mathrm{spikes/s}$. For supra-threshold stimuli, the firing-rate response grows with increasing sound intensity and saturates at $f_{max} = 250\,\mathrm{spikes/s}$. The resulting AN rate-intensity functions are shown in Fig. 1b (black line).

As our tinnitus subjects suffer from noise-induced hearing loss, the properties of the model AN are adjusted to capture the effects of noise-induced damage to inner and outer hair cells of the cochlea on AN activity (Liberman, 1984; Liberman and Dodds, 1984; Liberman and Kiang, 1984; Heinz and Young, 2004). Thus, for each frequency channel, we set the response threshold I_{th} of the AN fiber population to the corresponding hearing threshold of the subject's audiogram, and we decrease the spontaneous firing rate f_{sp} in proportion to the threshold increase: $f_{sp}(I_{th}) = f_{sp} \cdot (1 - I_{th}/120\,\mathrm{dB})$. The resulting population rate-intensity functions for different degrees of threshold elevation are shown in Fig. 1b (gray lines). To obtain the hearing thresholds at frequencies between the test tones of the audiometer, we linearly interpolate the audiograms.

The mean firing rates of the AN fibers in each frequency channel can be calculated from the distribution of sound intensities and the AN response functions. Noise-induced hearing loss decreases the mean firing rate in proportion to the degree of cochlear damage (Fig. 1c, details can be found in Schaette and Kempter, 2006).

Dorsal Cochlear Nucleus Model and Homeostatic Plasticity

The brainstem stage of our model is based on the minimal circuit that has been proposed for the DCN (Young and Davis, 2002), in which projection neurons (PNs) are inhibited by wide-band inhibitor (WBI) neurons and type II neurons. We refer to type II neurons as narrow-band inhibitor neurons, due to their function of providing inhibition for narrow-band stimuli only. All neurons of the minimal circuit receive excitatory input from the ipsilateral AN (Fig. 1). In the following, we briefly describe the main properties of the DCN model. Details can be found in Schaette and Kempter (2008).

Model for Wide-Band Inhibitor Neurons: WBI neurons strongly respond to broad-band noise, but only weakly to pure tones. In our model, a WBI neuron receives input from ten frequency channels firing with rates $f_1, f_2, \ldots, f_{10}$. The output firing-rate response w is given by a threshold-linear function W,

$$w = W(f_1, f_2, \ldots, f_{10}) = \left[\frac{1}{10} \sum_{\mathrm{i}=1}^{10} f_\mathrm{i} - \theta_\mathrm{w} \right]_+ , \tag{3}$$

where $[\ldots]_+$ denotes positive rectification, and $\theta_\mathrm{w} = 100$ spikes/s is the firing threshold.

Model for Narrow-Band Inhibitor Neurons: Our model for a narrow-band inhibitor (NBI) neuron is based on the responses of type II neurons of the DCN. Type II neurons are narrowly tuned; they respond strongly to pure tones but only weakly to broad-band noise. They receive excitation from the ipsilateral AN and are inhibited by WBI neurons. The output of the model NBI neuron is described by a threshold-linear response function N with a firing threshold $\theta_\mathrm{n} = 100$ spikes/s. Its firing rate n in response to AN input from a single frequency channel firing at rate f and WBI input at rate w is

$$n = N(f, w) = [f - g_\mathrm{nw} w - \theta_\mathrm{n}]_+ . \tag{4}$$

The gain factor g_nw determines the strength of the inhibition from the WBI neuron; it is set to $g_\mathrm{nw} = 1.5$ to ensure that the NBI neuron does not respond to broad-band noise.

Model for Projection Neurons: In our model, a PN receives excitatory input from a single AN frequency channel, and it is inhibited by a WBI and an NBI neuron. The PN and the NBI neurons receive excitatory input from AN fibers of the same frequency channel, and both neurons are also inhibited by the same WBI neuron (Fig. 1a). The gain factors g_w and g_n for inhibition from the WBI and the NBI neuron, respectively, determine the response characteristics of the PN (Schaette and Kempter, 2008). For the response function R of the PN, we choose

a hyperbolic tangent with positive rectification as this is a saturating function with convenient analytical properties. With a firing threshold of 0 spikes/s, the PN's firing rate response r is given by

$$r = R(f,w) = r_{\text{high}} \tanh\left(\frac{[f - g_{\text{w}} w - g_{\text{n}} N(f,w)]_+}{r_{\text{high}}}\right), \tag{5}$$

where f is the firing rate of the afferent AN fiber population, w is the firing rate of the WBI neuron, and $r_{\text{high}} = 300$ spikes/s is the maximum possible firing rate of the PN. The firing rate n of the NBI neuron is given as $n = N(f,w)$ as it depends on the same f and w as the PN's response due to their shared input.

Homeostatic Plasticity: We consider homeostasis through global scaling of synapse strengths, which is implemented through a homeostasis factor h: The gain of excitatory inputs is multiplied with h, and the gain of inhibitory inputs is divided by h to account for the opposite regulation of the strengths of excitatory and inhibitory inputs, as observed in experiments (Turrigiano et al., 1998; Kilman et al., 2002). The response r of a PN in dependence upon the value of the homeostasis factor h is then given by (Schaette and Kempter, 2008)

$$r = R(f,w,h) = r_{\text{high}} \tanh\left(\frac{[h \cdot f - g_{\text{w}} \cdot w/h - g_{\text{n}} \cdot N(f,w)/h]_+}{r_{\text{high}}}\right). \tag{6}$$

The mean firing rate can thus be regulated by changing h. The value of h is limited to the range of $[1/h_{\max}, h_{\max}]$ to account for physiological constraints on synaptic strength. If not stated otherwise, we use $h_{\max} = 3$.

We assume that the mean firing rates of the DCN PNs are stabilized at a certain target mean rate r^* by homeostatic plasticity. For each PN, r^* is the mean rate obtained for input from an undamaged cochlea and $h = 1$. In this case, equation (6) equals equation (5). For a damaged cochlea, the required change of h to restore the mean rate to its target level is determined numerically.

Lateral-Inhibition Layer and Tinnitus Pitch Prediction

We added a lateral-inhibition layer to our computational model because this is a general feature of information processing in the brain. The lateral-inhibition layer simplifies the estimation of pitch and enables us to compare the homeostasis model with models based on lateral inhibition only. The neurons of the lateral-inhibition layer receive excitatory input from the corresponding PNs of the DCN stage (Fig. 1a), and they are connected by inhibitory synapses. The pattern as well as the strength of the inhibitory connections are contained in the connection matrix $\mathbf{W}$, with the matrix component $w_{\text{ij}} \leq 0$ representing the strength of the synapse from a neuron in frequency channel j to a neuron in frequency channel i. We assume a threshold-linear response

function for the neurons in the lateral-inhibition layer. Thus, the activity $\vec{a} = (a_1, a_2, \ldots, a_{61})^{\mathrm{T}}$ of all neurons in the lateral-inhibition layer is determined by the condition

$$\vec{a} = [\vec{r} + \mathbf{W} \cdot \vec{a}]_+, \tag{7}$$

with the vector $\vec{r} = (r_1, r_2, \ldots, r_{61})^{\mathrm{T}}$ of the firing rates of the DCN PNs. The upper index 'T' denotes transposition so that $\vec{r}$ is a column vector.

We choose a unimodal distribution of inhibitory projections with symmetric inhibition toward lower and higher frequencies,

$$w_{\mathrm{ij}} = \begin{cases} -w_{\max} \cdot \frac{1}{2}\left[1 + \cos\left(\pi(i-j)/\sigma\right)\right] & \text{for } |i-j| \leq \sigma \\ 0 & \text{otherwise,} \end{cases} \tag{8}$$

where $w_{\max}$ denotes the maximum strength of the inhibitory synapse, and σ is the width of the arborization pattern of the inhibitory connections. We set the maximum strength to $w_{\max} = 0.8$ and the width to $\sigma = 5$ frequency channels. These values ensure efficient sharpening of peaks without the occurrence of pronounced side lobes (Fig. 2f). For the model with lateral inhibition only, the width is increased to $\sigma = 10$ frequency channels to reliably create peaks from the profiles of AN or DCN spontaneous firing rates after hearing loss (Fig. 2c,d)

In the absence of acoustic stimulation, the PNs of the model DCN fire at constant rate $\vec{r}_{\mathrm{sp}}$. We obtain the steady-state activity $\vec{a}_{\mathrm{sp}}$ of the neurons in the lateral-inhibition layer by numerically solving equation (7) with $\vec{r} = \vec{r}_{\mathrm{sp}}$ and $\vec{a} = \vec{a}_{\mathrm{sp}}$. The model tinnitus pitch is then derived from $\vec{a}_{\mathrm{sp}}$. We assume that the dominant pitch of the tinnitus sensation is determined by the characteristic frequency of the neuron with the highest spontaneous firing rate in the lateral-inhibition layer.

Evaluation of Pitch Prediction Performance

The error E of tinnitus pitch prediction is quantified using the root-mean-square deviation (in octaves) of the tinnitus frequencies p_{i} (in kHz), as predicted by the model for ear $i\,(i = 1, \ldots, n)$, from the pitch matching results t_{i} (in kHz) of the n ears:

$$E = \sqrt{\frac{1}{n}\sum_{i=1}^{n}\left[\log_2(p_{\mathrm{i}}/t_{\mathrm{i}})\right]^2}. \tag{9}$$

The bias B of pitch prediction is evaluated by computing the deviation of the mean predicted tinnitus pitch $\mu_{\mathrm{p}} = \frac{1}{n}\sum_i \log_2 p_{\mathrm{i}}$ from the mean observed tinnitus pitch $\mu_{\mathrm{t}} = \frac{1}{n}\sum_i \log_2 t_{\mathrm{i}}$:

$$B = \mu_{\mathrm{p}} - \mu_{\mathrm{t}}. \tag{10}$$

To assess the correlation between predicted and observed tinnitus pitch, we calculate the linear correlation coefficient C:

$$C = \frac{\mathrm{Cov}(p,t)}{\sigma_\mathrm{p}\sigma_\mathrm{t}}, \tag{11}$$

with the covariance given by $\mathrm{Cov}(p,t) = \frac{1}{n-1}\sum_i \log_2 p_\mathrm{i} \cdot \log_2 t_\mathrm{i} - \mu_\mathrm{p}\,\mu_\mathrm{t}$. The variances of predicted and observed tinnitus pitch are $\sigma_\mathrm{p}^2 = \frac{1}{n-1}\sum_i \left(\log_2 p_\mathrm{i} - \mu_\mathrm{p}\right)^2$ and $\sigma_\mathrm{t}^2 = \frac{1}{n-1}\sum_i \left(\log_2 t_\mathrm{i} - \mu_\mathrm{t}\right)^2$.

The implementation and evaluation of the model were done using MATLAB from the MathWorks Inc., Natick, Massachusetts.

Results

In this study, we present a model that reproduces tinnitus-related activity patterns in the auditory system after hearing loss, which allows us to estimate the tinnitus pitch from an audiogram. This phenomenological model comprises the auditory nerve (AN), the brainstem, and a stage with recurrent lateral inhibition as observed in higher auditory structures like for example the inferior colliculus and the auditory cortex (Fig. 1a, see Methods for details).

In the AN stage of the model, we capture the effects of noise-induced hearing loss on AN activity by adjusting the shape of the rate-intensity functions (Fig. 1b). The brainstem stage of the model resembles the basic circuit of the dorsal cochlear nucleus (DCN, see Young and Davis, 2002, for a review), and the model neurons reproduce salient features of the responses of DCN neurons (Schaette and Kempter, 2008). After hearing loss through cochlear damage, homeostatic plasticity adjusts the effective response gain of the model DCN projection neurons (PNs) in order to stabilize their mean firing rates at a certain target level. This stabilization can lead to the development of increased spontaneous firing rates, which we interpret as neural correlates of tinnitus (Schaette and Kempter, 2006, 2008). The model tinnitus pitch is derived from the activity pattern of neurons in the lateral-inhibition layer. This lateral-inhibition layer is not meant to represent a specific region of the auditory system; its function is merely to demonstrate how lateral inhibition could amplify unevenness in the profile of spontaneous firing rates, giving rise to activity peaks that might underly tone-like tinnitus.

Predicting Tinnitus Pitch from Patients' Audiograms

Computational models of tinnitus should provide testable predictions of characteristics of tinnitus in human subjects or animal models of tinnitus. We thus test the ability of our model to predict tinnitus pitch from the audiograms of 24 tinnitus patients with noise-induced hearing loss and tone-like tinnitus (Fig. 2a). Figure 2b shows the audiograms of 3 example subjects; their perceived tinnitus pitch is indicated by downward arrows.

To predict the tinnitus pitch from an audiogram, we adjust the response properties of the model AN fibers in all frequency channels to the measured hearing loss. Specifically, we match the response threshold in each AN frequency channel to the hearing threshold obtained from the interpolated audiogram, and we set the spontaneous firing rate accordingly (Fig. 1b and Methods), as observed after noise-induced damage to the stereocilia of inner and outer hair cells (Liberman, 1984; Liberman and Dodds, 1984; Liberman and Kiang, 1984; Heinz and Young, 2004). Resulting activity profiles of the model AN are shown in Fig. 2c. The mean and the spontaneous firing rates are reduced in the AN frequency channels that are affected by the hearing loss, which concerns predominantly the high-frequency range in our examples. Thus, hearing loss reduces the excitatory input from the AN to the higher stages of the model, which

therefore also reduces the mean and spontaneous firing rates of the corresponding PNs in the DCN stage of the model (Fig. 2d).

In our model, we assume that the mean firing rates of PNs in the DCN are stabilized at a certain target level by homeostatic plasticity. A decrease in the mean firing rates after hearing loss then activates homeostasis in the affected PNs. We assume that homeostasis acts on the single-neuron level, i.e. each PN individually tries to stabilize its mean firing rate. To counteract the reduction of the mean firing rate of a PN after hearing loss, homeostasis increases the strength of the excitatory projections onto the PN and decreases inhibitory synaptic strengths, thus elevating the effective response gain.

An increase in the response gain of central auditory neurons through homeostatic plasticity after hearing loss can lead to hyperactivity (Schaette and Kempter, 2006, 2008). For example, the PNs in Fig. 2e that receive input from the damaged parts of the cochlea exhibit increased spontaneous firing rates. The degree to which the spontaneous firing rates are elevated depends on the severity of hearing impairment at this frequency channel.

Homeostatic plasticity is able to stabilize the mean firing rates of all DCN PNs at the target level for the first two subjects (left and middle columns in Fig. 2e). For the third subject (right column), the situation is slightly different. Hearing loss is more severe in the highest frequency channels, thus demanding an increased amount of homeostatic compensation. However, taking into account physiological constraints on synaptic strength, we impose an upper limit for homeostatic plasticity. As a consequence, homeostasis is saturated for the DCN PNs at characteristic frequencies at which hearing loss is severe enough, and the mean rates of these PNs remain below the target level. As a result, the spontaneous firing rate increases with increasing hearing loss until the saturation point is reached, and then decreases again.

The neurons of the lateral-inhibition layer, the next processing stage of the model, receive excitatory input from the PNs of the DCN stage. The input patterns of DCN spontaneous firing rates after homeostasis (Fig. 2e, red solid lines) lead to activity profiles with distinct peaks in the lateral-inhibition layer (Fig. 2f, red lines). The peaks are located at frequencies above the audiogram edge, where hearing is impaired; peaks are created through an amplification of patterns of DCN hyperactivity that developed in the frequency channels affected by hearing loss. If such peaks are interpreted as the basis for a tone-like tinnitus sensation, with a perceived pitch that corresponds to the characteristic frequency of the neuron with the highest firing rate, the model predicts tinnitus pitch (red upward arrows) close to the subjects' perceived pitch (downward errors in Fig. 2a).

This tinnitus pitch prediction procedure is applied to the audiograms from all 24 subjects. The distribution of predicted tinnitus pitch in the homeostasis model (Fig. 3a, bars with red outlines) matches the distribution of the observed tinnitus pitch (Fig. 3a, gray bars). The bias of model tinnitus pitch predictions is low: $B = -0.05$ octaves (see Methods). A scatter plot of

the model predictions versus the tinnitus pitch reported by the subjects is depicted in Fig. 3b. The correlation coefficient between predicted and observed pitch is $C = 0.49$ ($p = 0.0005$). For the pitch prediction error E, as quantified by the root-mean-square deviation (see Methods), we obtain $E = 0.60$ octaves, which is comparable to the uncertainty of tinnitus pitch matching with human subjects (Burns, 1984; Henry et al., 2004).

Predictions of a Tinnitus Model with Lateral Inhibition only are Systematically too Low

For comparison to our homeostasis model, we evaluate the performance of a model where tinnitus-related activity patterns are generated by lateral inhibition only, as proposed by Gerken (1996). In our model framework, this can be achieved by disabling homeostatic plasticity in the brainstem stage. We illustrate pitch prediction with the lateral-inhibition model for the three example patients: As before, the patients' noise-induced hearing loss (Fig. 2b) decreases the spontaneous firing rates of both the AN and DCN in the high-frequency range (Fig. 2c and d, solid lines). When such an activity profile with a steep drop is processed by a neuronal structure with lateral inhibition (but without homeostatic plasticity), an activity peak at the edge of the profile is created (Fig. 2f, blue lines). The most prominent activity peak is thus generated close to the audiogram edge, and thus the model predicts the tinnitus pitch around the audiogram edge frequency. However, the audiogram edge frequency is generally below the perceived tinnitus pitch (Henry et al., 1999; König et al., 2006), and thus the lateral-inhibition model predicts tinnitus pitch systematically too low (Fig. 3, blue color); the bias is $B = -1.47$ octaves, the correlation coefficient is $C = 0.37$ ($p = 0.01$), and the prediction error is $E = 1.62$ octaves. The performance of the lateral-inhibition model is worse than that of the homeostasis model.

The pitch prediction performance of the lateral-inhibition model is judged against a the performance of a very simple estimator of tinnitus pitch, which simply takes the frequency of the audiogram edge (see Methods). The bias of this estimator is $B = -1.48$ octaves, the prediction error is $E = 1.69$ octaves, and the correlation coefficient is $C = 0.30$ ($p = 0.04$). The performances of this edge-detection model and the lateral-inhibition model in predicting tinnitus pitch are similarly weak.

Our new model including homeostatic plasticity predicts tinnitus pitch much more accurately than the lateral-inhibition model or the model based on the audiogram edge. We conclude that models including homeostatic plasticity can considerably increase tinnitus-pitch prediction performance.

Successful Pitch Prediction Requires Hyperactivity

We now test the robustness of pitch prediction with respect to variation of model parameters. The most important parameters are the strengths of the inhibitory projections from the interneurons within the DCN, which determine the response properties of PNs (Schaette and Kempter, 2008). These parameters also control whether homeostatic plasticity after hearing loss can lead to hyperactivity. In the model used so far (Figures 2 and 3), the corresponding gain factors of inhibition were set to $g_{\mathrm{w}} = 0.6$ and $g_{\mathrm{n}} = 1.3$ (see Fig. 1a and Methods), and the resulting PNs could become hyperactive after hearing loss. We now systematically vary the values of g_{w} (from 0 to 1.5) and g_{n} (from 0 to 3) to determine their influence on pitch prediction.

We find low prediction errors E (Fig. 4a) and high correlation coefficients C (not shown) when PNs receive weak to moderate inhibition. The lowest prediction error is $E = 0.59$ octaves, and the highest correlation is $C = 0.51$ (for $g_{\mathrm{w}} = 0.2$ and $g_{\mathrm{n}} = 2$). Moreover, for a wide range of gain factors (area left of the black contour line line at 1 octave in Fig. 4a), prediction errors of the homeostasis model are reasonable and much lower than the errors $E = 1.62$ octaves and $E = 1.69$ octaves obtained from the lateral-inhibition model and the edge-detection model, respectively. For strong inhibition (high values of both g_{w} and g_{n}, area right of the black line in Fig. 4a), on the other hand, prediction errors are high.

To show that the performance of pitch prediction is linked to hyperactivity after hearing loss, we consider the case of 60 dB noise-induced hearing loss in all frequency channels. The resulting spontaneous activity of DCN PNs is shown in Fig. 4b, again as a function of the inhibitory gain factors g_{w} and g_{n}. For a wide range of gain factors we observe hyperactivity (area left of the black contour line at 50 spikes/s in Fig. 4b). We note that this parameter region largely overlaps with the parameter region in Fig. 4a for which tinnitus pitch is predicted with low error. On the other hand, the parameter region where pitch predictions are inconsistent with the data coincides with the parameter region where PNs do not become hyperactive – the spontaneous firing rate can even be decreased after hearing loss and homeostasis (areas right of the contour lines in Figs. 4a and b). We conclude that hyperactivity is required for accurate pitch prediction.

In our model, we assume that homeostatic plasticity scales synaptic strength. However, physiological constraints limit the amount of scaling. We have accounted for this constraint by limiting the homeostasis factor h (see Methods) to a certain maximum value $h_{\max}$, which was set to $h_{\max} = 3$ in the model used so far. The value of $h_{\max}$ determines at which degree of hearing loss the saturation point of homeostasis is reached, and it therefore also controls whether hyperactivity is generated or not. Figure 4c shows the resulting spontaneous activity as a function of the degree of hearing loss – for several values of $h_{\max}$. When $h_{\max}$ is increased, homeostasis saturates at a higher degree of hearing loss, and the maximum of the spontaneous firing rate is increased. In the model without homeostasis ($h_{\max} = 1$), which corresponds to the

lateral-inhibition model, the spontaneous firing rate decreases with increasing hearing loss.

We finally assess the effect of the model parameter $h_{\max}$ on pitch prediction performance for our sample of patients. In particular, we determine the minimum prediction error from the results obtained for all combinations of g_{w} and g_{n} (Fig. 4d). We find that for $h_{\max} \geq 1.5$ the minimum prediction error is lower than 1 octave. For $h_{\max} \geq 3$, the minimum prediction error stays constant. Thus, if $h_{\max}$ is high enough, and hyperactivity can develop in the model, fairly accurate predictions of tinnitus pitch can be obtained.

Model Predictions for Tinnitus Treatment

With our computational model, we have demonstrated how hearing loss could lead to neuronal hyperactivity and tinnitus through a central compensation for decreased AN activity. Thus, a complete renormalization of AN activity, for example through a hypothetical perfect hearing aid, could completely abolish tinnitus in the model; moreover, a simpler strategy of matched-noise stimulation is also sufficient (Schaette and Kempter, 2006, 2008). We need to assume, however, that there are no cochlear dead regions (Moore et al., 2000), i.e., regions where inner hair cells are completely lost. Cochlear dead regions would preclude acoustic stimulation of the corresponding AN fibers.

Most current hearing aids provide little to no amplification above 5-6 kHz (Moore, 2007), and similar limitations apply to noise generators that are worn behind the ear. Central auditory neurons that are sensitive to frequencies above this cut-off frequency of the stimulation device thus remain unstimulated. Additional acoustic stimulation with a hearing aid could therefore create an effective audiogram edge beyond 5-6 kHz, and the stimulation might simply shift the tinnitus. We evaluate this scenario in our model for the second subject in Fig. 2. The audiogram is shown again in the top panel of Fig. 5a. Without additional acoustic stimulation, there is hyperactivity in the model DCN, and the activity pattern in the lateral-inhibition layer shows a distinct peak at 4 kHz.

We first consider stimulation with a hypothetical perfect hearing aid that completely restores AN activity to normal levels, but only up to its cut-off frequency of 6 kHz. The black line in Fig. 5b (top panel) shows the effective audiogram that is created by this device. After prolonged stimulation, homeostasis adapts the gain factors in the model DCN. The resulting pattern of spontaneous firing rates along the tonotopic axis of the DCN still shows increased spontaneous firing rates for neurons with characteristic frequencies above 6 kHz (Fig. 5b, middle panel). In the lateral-inhibition layer, the resulting activity pattern has a pronounced peak at approximately 7 kHz (Fig. 5b, bottom panel), which is similar in magnitude to the tinnitus peak without hearing aid use (Fig. 5a, bottom panel); the stimulation with the hearing aid has just shifted the pitch of the tinnitus.

To avoid the problem of just shifting tinnitus pitch by means of a hearing aid with a sharp cut-off frequency, we propose an alternative stimulation strategy that uses the hearing aid to flatten the audiogram. The gains of the hearing aid are to be set such that the resulting effective audiogram has a smooth transition from normal hearing to hearing loss. In the example shown in Fig. 5c (black line in the top panel), the transition range spans more than two octaves, and the effective hearing level has a shallow slope. After prolonged use of this device, the spontaneous firing rates in the model DCN are still slightly elevated in the high-frequency range. However, the resulting pattern of spontaneous firing rates along the tonotopic axis is smooth. As a consequence, the activity in the lateral-inhibition layer does not display a pronounced activity peak (Fig. 5c, bottom panel). This scenario corresponds to a reduction of tinnitus compared to Figs. 5a and b.

Discussion

We have presented a computational model that predicts changes in the spontaneous firing rates of neurons in the central auditory system after hearing loss, and we applied the model to the audiograms of tinnitus patients with moderate to severe noise-induced hearing loss in the high-frequency range and tone-like tinnitus. Because the etiology of hearing loss was known, we could model the subjects' hearing loss based on animal studies on how acoustic trauma influences auditory nerve (AN) activity (see, e.g., Liberman, 1984; Liberman and Dodds, 1984; Liberman and Kiang, 1984; Heinz and Young, 2004). The resulting hyperactivity patterns in the model brainstem were consistent with the measured pitch of the tinnitus sensation, and the tinnitus-pitch prediction error was close to the error of tinnitus pitch measurements in patients (Burns, 1984; Henry et al., 2004). We note that the values of the model parameters were constrained by physiology; there were no free parameters that needed to be tuned, and the performance of the model was robust against variation of the most important parameter values.

In our model, we assumed that the mean firing rates of projection neurons (PNs) in the dorsal cochlear nucleus (DCN) are stabilized by homeostatic plasticity. In the healthy auditory system, homeostatic plasticity could help to ensure that auditory neurons are active within the right range of firing rates, independent of the prevailing acoustic environment. Homeostatic plasticity in auditory neurons might also prevent us from perceiving spontaneous neuronal activity as sound. For pathologically altered processing in the cochlea, however, this plasticity mechanism could also have detrimental effects. After sensorineural hearing loss, for example, homeostatic plasticity can lead to the development of increased spontaneous firing rates of PNs in the DCN (Schaette and Kempter, 2006, 2008). Such hyperactivity was crucial for predicting tinnitus pitch: predictions were reasonable only if model neurons became hyperactive after hearing loss. In contrast, for parameter combinations that resulted in absence of hyperactivity, the computed tinnitus pitch was not consistent with patient data; and when homeostasis was disabled, the predicted tinnitus pitch was systematically too low (Fig. 3). Thus, we could demonstrate that hyperactivity through homeostatic plasticity is important to generate a neuronal activity pattern in the model that is consistent with the observed tinnitus pitch.

Our model is based on results from animal studies, in particular those on rodents, that demonstrated hyperactivity of DCN neurons *in vivo* after acoustic trauma (see, e.g. Kaltenbach and McCaslin, 1996; Brozoski et al., 2002; Kaltenbach et al., 2004). *In vivo*, hyperactive neurons were found in the fusiform cell layer (Brozoski et al., 2002), but a direct identification of the cell type *in vitro* has proven difficult, as spontaneous firing rates were not increased in a slice preparation (Chang et al., 2002). In cats, on the other hand, DCN hyperactivity after acoustic trauma was not observed (Ma and Young, 2006). We have shown previously that this discrepancy could be explained through species-specific differences in DCN response proper-

ties (Schaette and Kempter, 2008). For the prediction of tinnitus pitch from human audiograms, a DCN model with moderate inhibition was most successful, and the model parameters correspond to DCN neuron response characteristics that are more prevalent in rodents than in cats. However, the DCN need not be the only generator of tinnitus in the auditory system because ablation of the DCN after acoustic trauma did not abolish behavioral signs of tinnitus (Brozoski and Bauer, 2005). Moreover, following manipulations that induce tinnitus, increased spontaneous firing rates have also been found in the inferior colliculus of mice (Ma et al., 2006) and the auditory cortex of cats (Noreña and Eggermont, 2003). In principle, homeostatic plasticity could lead to increased spontaneous firing rates in a variety of neuron types along the auditory pathway, and the resulting hyperactivity hotspots at various stages of the auditory system might contribute to the tinnitus sensation.

Changes that are reminiscent of homeostatic plasticity have been observed at various stages of the auditory pathway after cochlear damage: In the auditory cortex of gerbils, bilateral cochlear ablation elevated neuronal excitability, increased the amplitudes of evoked excitatory postsynaptic currents (EPSCs), but decreased the amplitudes of evoked inhibitory responses (Kotak et al., 2005). Similar changes were also observed in the inferior colliculus of gerbils, where bilateral deafening led to increased EPSC amplitudes and increased equilibrium potentials of inhibitory synaptic currents (Vale and Sanes, 2002). Increased EPSC amplitudes were also observed in the anteroventral cochlear nucleus of congenitally deaf mice in response to electrical stimulation of the AN (Oleskevich and Walmsley, 2002). After unilateral ablation of the cochlea of guinea pigs, evoked glycine release (Suneja et al., 1998b) and glycine receptor binding (Suneja et al., 1998a) declined in the DCN, indicating weakened glycinergic inhibition. Furthermore, after bilateral cochlear ablation, decreased expression of potassium channels was found in the cochlear nucleus (Holt et al., 2006) and the inferior colliculus (Cui et al., 2007), indicating that the excitability of neurons in these nuclei might have been increased. All these findings indicate that homeostatic plasticity regulates neuronal activity throughout the auditory pathway.

We chose to model the DCN because the circuitry and the responses of the neurons of this nucleus are well characterized, which enabled us to derive a model that is constrained by physiology. Our results, however, are not limited to the DCN. The model can be adapted to describe circuits in other brain regions by adjusting, for example, the strengths of feedforward inhibitory connections, a scenario that we explored in Figs. 4a and b. Other modeling studies have shown that homeostatic compensation for decreased excitatory input can lead to hyperactivity in cortex-like networks (Houweling et al., 2005; Dominguez et al., 2006). Concerning the level of modeling, our approach has the advantage of being as simple as possible to exhibit the consequences of homeostatic plasticity in the auditory system and to demonstrate how hyperactivity could relate to tinnitus. Our model can be analytically treated, it does not require

fitting of free parameters, and it does not rely on extensive numerical simulations whose results may be difficult to interpret.

Given that homeostatic plasticity acts at various stages along the auditory pathway, one might argue that hyperactivity generated in DCN neurons is reduced to normal levels at higher processing stages. However, this is not necessarily the case because the fraction of time a neuron spends firing at its spontaneous rate cannot be decreased by homeostasis or other plasticity mechanisms; this fraction is fixed by the response threshold of AN fibers (Schaette and Kempter, 2006). As a consequence, hearing loss increases the contribution of spontaneous activity to the mean firing rate of neurons at all stages of the auditory pathway. Thus, for neurons that have a target mean rate above their healthy spontaneous firing rate, we expect that homeostatic plasticity leads to hyperactivity (Schaette and Kempter, 2008).

The consequences of homeostasis acting in a network of neurons might also depend on which types of neurons employ this mechanism. In our model, homeostasis stabilizes the firing rates of only one neuron type, the PNs of the DCN. We have also implemented a variant of the model where, in addition to the PNs, also the mean firing rates of the inhibitory interneurons of the DCN were stabilized by homeostatic plasticity. However, this model variant did not lead to hyperactivity in the inhibitory interneurons; in the PNs, however, hyperactivity was even slightly more pronounced. The resulting pitch prediction performance of this model variant was similar to that of the model with homeostasis in the PNs only, further demonstrating that our results do not depend on details of the implementation of homeostasis.

To estimate a tinnitus pitch, we associated profiles of spontaneous neuronal activity along the tonotopic axis of a neuronal structure (lines in Figs.2 d and e) with a certain pitch. To extract a pitch from a profile, we used a lateral-inhibition layer that exaggerates edges of the profile and creates peaks of activity. This procedure may be related to the edge-pitch phenomenon in psychophysics, where a bandpass broadband acoustic signal produces a tonal pitch percept at the spectral edge of the signal (Kohlrausch and Houtsma, 1992).

The evaluation of tinnitus pitch in our model relies on the assumption of a rate-place code, i.e. the dominant pitch is determined by the location (along the tonotopic axis) of the neuron with the highest firing rate. This assumption is in accordance with the tonotopic arrangement of neurons in the auditory pathway, and, in particular, of pitch-sensitive neurons in the auditory cortex (Bendor and Wang, 2005). A representation of tinnitus pitch in the temporal pattern of the neuronal discharge (with spikes being phase-locked to the perceived tinnitus frequency) is less likely, as tinnitus is usually a high-pitched sensation that is matched to comparison tones above 2 kHz by most subjects (Henry et al., 1999). For such high frequencies, temporal coding of pitch using interspike-interval representations is not to be expected.

A tinnitus sensation may be complex and consist of multiple components instead of just a pure tone. As a consequence, tinnitus spectra that were obtained when subjects were asked to

judge the contribution of comparison tones to their tinnitus sensation usually spanned a broad frequency range (Noreña et al., 2002). For audiogram shapes characteristic of noise-induced hearing loss, our model generates spontaneous activity patterns that are elevated over broad frequency ranges, and there can even be more than one peak (Fig. 2f). Such patterns could constitute the basis for complex tinnitus sensations. However, our results are limited by the low frequency resolution of the available audiometric data, and therefore we cannot predict the quality or timbre of the tinnitus sensation.

For comparison to the homeostasis model, we have re-implemented the lateral-inhibition model of tinnitus generation as proposed by Gerken (1996). In this model, discontinuities of the spontaneous AN activity along the tonotopic axis after hearing loss are exaggerated by lateral inhibition in higher auditory structures. After noise-induced hearing loss, the lateral-inhibition model generates tinnitus-related activity peaks at the audiogram edge, which produces the greatest discontinuity in AN activity. Because tinnitus pitch is generally well above the audiogram edge (Henry et al., 1999; König et al., 2006), the lateral-inhibition model predicts tinnitus pitch systematically too low (Fig. 3). The main difference between the lateral-inhibition model and our full model is activity stabilization through homeostatic plasticity. Homeostatic plasticity inverts the profile of spontaneous activity, which can be seen in the examples shown in Figure 2: Before homeostasis, the spontaneous activity is largest at low frequencies, where we have little hearing loss (full lines in Fig. 2d). After homeostasis, the spontaneous activity is largest at high frequencies at which hearing is impaired (full lines in Fig. 2e). The activity profile is thus inverted, and the profile's edge is shifted to higher frequencies. Lateral inhibition then exaggerates this edge, and the resulting peak is in the region where hearing is impaired, often closely matching the subject's perceived pitch. This intuitive picture explains why homeostatic plasticity is an essential ingredient for obtaining tinnitus pitch predictions that are consistent with subject data.

A future perspective for modeling tinnitus would be to combine our elementary approach with a detailed model of cochlear processing. A more realistic model of cochlear processing as a front-end to an extended, spike-based model of auditory processing and tinnitus development would enable us to present a variety of acoustic stimuli and to determine their effect on tinnitus-related hyperactivity. For example, masking curves could be obtained for the model tinnitus and be compared to those measured with tinnitus subjects. Moreover, we could implement a personalized tinnitus model for each tinnitus subject and determine the effects of various treatment strategies like for example hearing aids and masking devices with different settings. However, detailed high-resolution audiometry and psychophysical tests to characterize the status of the cochlear hair cells would be an essential prerequisite for such a project. We might then also be able to evaluate which kinds and characteristics of hearing loss lead to tinnitus. Another possible extension of the model would be to incorporate long-term potentia-

tion and depression of synaptic strength. This form of plasticity might be especially interesting in the context of somatic tinnitus, as in the DCN this mechanism seems to be exclusive to the parallel fiber system that conveys somatosensory information to DCN neurons: the synapses of parallel fibers onto fusiform and cartwheel cells have been shown to be plastic (Fujino and Oertel, 2003; Tzounopoulos et al., 2004), whereas synapses of AN fibers onto fusiform cells could not be influenced by changes in activity on short time scales (Fujino and Oertel, 2003).

In this article, we argued that tinnitus-related hyperactivity after hearing loss can be a consequence of a homeostatic compensation for decreased AN activity. This view suggests that it should be possible to reduce tinnitus that is caused by hearing loss by increasing AN activity through additional acoustic or electric stimulation. Additional acoustic stimulation could be delivered, for example, through a hearing aid or a noise-device, and stimuli adjusted to the hearing loss might be most effective for treating tinnitus (Schaette and Kempter, 2006, 2008). This idea is supported by findings that the spontaneous firing rates of cortical neurons can be altered through prolonged stimulation *in vitro* (Johnson and Buonomano, 2007) and *in vivo* (Quairiaux et al., 2007), and that exposure to an enhanced acoustic environment after acoustic trauma can prevent the development of increased spontaneous firing rates (Noreña and Eggermont, 2006). In humans, additional acoustic stimulation can influence the gain of central auditory structures, leading to a reduction of the perceived loudness of sound events (Formby et al., 2003; Noreña and Chery-Croze, 2007). Furthermore, tinnitus can be reduced through direct electric stimulation of the cochlear nerve (Holm et al., 2005), and stimulation through a cochlear implant can produce residual inhibition of tinnitus that lasts for more than 12 hours (Heyning et al., 2008).

Any acoustic-stimulation strategy for tinnitus treatment requires that AN fibers still respond to sound. If the tinnitus of a patient is associated with a cochlear dead region where inner hair cells are completely lost, acoustic stimulation of the AN fibers is impossible. Moreover, acoustic stimulation might be ineffective for tinnitus that is not linked to hearing loss, like for example pulsatile tinnitus. Acoustic-stimulation strategies are also limited by the restricted frequency range of current hearing aids and noise generators that are worn behind the ear; the upper cut-off frequency of the devices might even create an artificial audiometric edge, and the tinnitus pitch might be just shifted to a frequency above this edge. An artificial audiometric edge can be avoided when the hearing aid is adjusted such that it leads to a smooth enough transition from good to impaired hearing, i.e. generates a shallow audiogram slope. Shallow audiogram slopes are less likely to be associated with tinnitus than steep audiogram slopes (König et al., 2006).

To conclude, our results provide a conceptual framework for understanding the origin of some forms of tinnitus, and this understanding might lead to new treatment strategies.

Acknowledgments

We would like to thank Ovidiu König and Manfred Gross for providing us with the patient data used in this study, and Christian Leibold for most helpful discussions on this work.

Grants

This research was supported by the Deutsche Forschungsgemeinschaft (DFG) through the Emmy Noether Programm (Ke 788/1-4), the SFB 618 “Theoretical Biology”, and the Bundesministerium für Bildung und Forschung (Bernstein Center for Computational Neuroscience Berlin, 01GQ0410; Bernstein Collaboration “Temporal Precision”, 01GQ07102).

Abbreviations

AN, auditory nerve
DCN, dorsal cochlear nucleus
EPSC, excitatory postsynaptic current
NBI, narrow-band inhibitor
PN, projection neuron
WBI, wide-band inhibitor

Bibliography

D. Bendor and X. Wang. The neuronal representation of pitch in primate auditory cortex. *Nature*, 436:1161–1165, 2005.

T. J. Brozoski and C. A. Bauer. The effect of dorsal cochlear nucleus ablation on tinnitus in rats. *Hear. Res.*, 206: 227–236, 2005.

T. J. Brozoski, C. A. Bauer, and D. M. Caspary. Elevated fusiform cell activity in the dorsal cochlear nucleus of chinchillas with psychophysical evidence of tinnitus. *J. Neurosci.*, 22:2383–2390, 2002.

E.M. Burns. A comparison of variability among measurements of subjective tinnitus and objective stimuli. *Audiology*, 23:426–440, 1984.

H. Chang, K. Chen, J. A. Kaltenbach, J. Zhang, and D. A. Godfrey. Effects of acoustic trauma on dorsal cochlear nucleus neuron activity in slices. *Hear. Res.*, 164:59–68, 2002.

Y. L. Cui, A. G. Holt, C. A. Lomax, and R. A. Altschuler. Deafness associated changes in two-pore domain potassium channels in the rat inferior colliculus. *Neuroscience*, 149:421–433, 2007.

M. Dominguez, S. Becker, I. Bruce, and H. Read. A spiking neuron model of cortical correlates of sensorineural hearing loss: Spontaneous firing, synchrony, and tinnitus. *Neural Comput.*, 18:2942–2958, 2006.

C. Formby, L. P. Sherlock, and S. L. Gold. Adaptive plasticity of loudness induced by chronic attenuation and enhancement of the acoustic background. *J. Acoust. Soc. Am.*, 114:55–58, 2003.

K. Fujino and D. Oertel. Bidirectional synaptic plasticity in the cerebellum-like mammalian dorsal cochlear nucleus. *Proc. Natl. Acad. Sci. USA*, 100:265–270, 2003.

G. M. Gerken. Central tinnitus and lateral inhibition: an auditory brainstem model. *Hear. Res.*, 97:75–83, 1996.

M. G. Heinz and E. D. Young. Response growth with sound level in auditory nerve fibers after noise-induced hearing loss. *J. Neurophysiol.*, 91:784–794, 2004.

J. A. Henry, M. Meikle, and A. Gilbert. Audiometric correlates of tinnitus pitch: insights from the Tinnitus Data Registry. In J. Hazell, editor, *Proceedings of the Sixth International Tinnitus Seminar*, pages 51–57. The Tinnitus and Hyperacusis Centre, London, 1999.

J. A. Henry, C. L. Flick, A. Gilbert, R. M. Ellingson, and S. A. Fausti. Comparison of manual and computer-automated procedures for tinnitus pitch-matching. *J. Rehabil. Res. Dev.*, 41:121–138, 2004.

P. Van de Heyning, K. Vermeire, M. Diebl, P. Nopp, I. Anderson, and D. De Ridder. Incapacitating unilateral tinnitus in single-sided deafness treated by cochlear implantation. *Ann. Otol. Rhinol. Laryngol.*, 117:645–652, 2008.

A. F. Holm, M. J. Staal, J. J. A. Mooij, and F. W. J. Albers. Neurostimulation as a new treatment for severe tinnitus: a pilot study. *Otol. Neurootol.*, 26:425–428, 2005.

A. G. Holt, M. Asako, R. K. Duncan, C.A. Lomax, J. M. Juiz, and R. A. Altschuler. Deafness associated changes in expression of two-pore domain potassium channels in the rat cochlear nucleus. *Hear. Res.*, 216-217:146–153, 2006.

A. R. Houweling, M. Bazhenov, I. Timofeev, M. Steriade, and T. J. Sejnowski. Homeostatic synaptic plasticity can explain post-traumatic epileptogenesis in chronically isolated neocortex. *Cereb. Cortex*, 15:834–845, 2005.

H. A. Johnson and D. V. Buonomano. Development and plasticity of spontaneous activity and up states in cortical organotypic slices. *J. Neurosci.*, 27:5915–5925, 2007.

J. A. Kaltenbach and D. L. McCaslin. Increases in spontaneous activity in the dorsal cochlear nucleus following exposure to high intensity sound: a possible neural correlate for tinnitus. *Audit. Neurosci.*, 3:57–78, 1996.

J. A. Kaltenbach, M. A. Zacharek, J. Zhang, and S. Frederick. Activity in the dorsal cochlear nucleus of hamsters previously tested for tinnitus following intense tone exposure. *Neurosci. Lett.*, 355:121–125, 2004.

V. Kilman, M. C. W. van Rossum, and G. G. Turrigiano. Activity deprivation reduces miniature IPSC amplitude by decreasing the number of postsynaptic $GABA_a$ receptors clustered at neocortical synapses. *J. Neurosci.*, 22: 1328–1337, 2002.

A. Kohlrausch and A. J. Houtsma. Pitch related to spectral edges of broadband signals. *Philos. Trans. R. Soc. Lond. B Biol. Sci.*, 29:375–382, 1992.

O. König, R. Schaette, R. Kempter, and M. Gross. Course of hearing loss and occurrence of tinnitus. *Hear. Res.*, 221:59–64, 2006.

V. C. Kotak, S. Fujisawa, F. A. Lee, O. Karthikeyan, C. Aoki, and D. H. Sanes. Hearing loss raises excitability in the auditory cortex. *J. Neurosci.*, 25:3908–3918, 2005.

M. C. Liberman. Single-neuron labeling and chronic cochlear pathology. I. Threshold shift and characteristic-frequency shift. *Hear. Res.*, 16:33–41, 1984.

M. C. Liberman and L. W. Dodds. Single-neuron labeling and chronic cochlear pathology. II. Stereocilia damage and alterations of spontaneous discharge rates. *Hear. Res.*, 16:43–53, 1984.

M. C. Liberman and N. Y. Kiang. Single-neuron labeling and chronic cochlear pathology. IV. Stereocilia damage and alterations in rate- and phase-level functions. *Hear. Res.*, 16:75–90, 1984.

W. L. Ma and E. D. Young. Dorsal cochlear nucleus response properties following acoustic trauma: response maps and spontaneous activity. *Hear. Res.*, 216-217:176–188, 2006.

W. L. Ma, H. Hidaka, and B. J. May. Spontaneous activity in the inferior colliculus of CBA/J mice after manipulations that induce tinnitus. *Hear. Res.*, 212:9–21, 2006.

A. R. Møller. Tinnitus: presence and future. In B. Langguth, B. Hajak, T. Kleinjung, T. Cacace, and A. R. Moller, editors, *Tinnitus: Pathophyiology and Treatment*, pages 3–16. Elsevier, Amsterdam, 2007.

B. C. Moore, M. Huss, D. A. Vickers, B. R. Glasberg, and J. L. Alcantara. A test for the diagnosis of dead regions in the cochlea. *Br. J. Audiol.*, 34:205–224, 2000.

B. C. J. Moore. *Cochlear Hearing Loss: Physiological, Psychological and Technical Issues*. John Wiley & Sons Ltd., Chichester, 2007.

C. Nicolas-Puel, R.L. Faulconbridge, M. Guitton, J. L. Puel, M. Mondain, and A. Uziel. Characteristics of tinnitus and etiology of associated hearing loss: a study of 123 patients. *Int. Tin. J.*, 8:37–44, 2002.

A. J. Noreña and S. Chery-Croze. Enriched acoustic environment rescales auditory sensitivity. *Neuroreport*, 18: 1251–1255, 2007.

A. J. Noreña and J. J. Eggermont. Changes in spontaneous neural activity immediately after an acoustic trauma: implications for neural correlates of tinnitus. *Hear. Res.*, 183:137–153, 2003.

A. J. Noreña and J. J. Eggermont. Enriched acoustic environment after noise trauma abolishes neural signs of tinnitus. *Neuroreport*, 17:559–563, 2006.

A. J. Noreña, C. Micheyl, S. Chery-Croze, and L. Collet. Psychoacoustic characterization of the tinnitus spectrum: implications for the underlying mechanisms of tinnitus. *Audiol. NeuroOtol.*, 7:358–369, 2002.

S. Oleskevich and B. Walmsley. Synaptic transmission in the auditory brainstem of normal and congenitally deaf mice. *J. Physiol.*, 540:447–455, 2002.

L. C. Parra and B. A. Pearlmutter. Illusory percepts from auditory adaptation. *J. Acoust. Soc. Am.*, 121:1632–1641, 2007.

C. Quairiaux, M. Armstrong-James, and E. Welker. Modified sensory processing in the barrel cortex of the adult mouse after chronic whisker stimulation. *J. Neurophysiol.*, 97:2130–2147, 2007.

L. E. Roberts, G. Moffat, M. Baumann, L. M. Ward, and D. J. Bosnyak. Residual inhibition functions overlap tinnitus spectra and the region of auditory threshold shift. *J. Assoc. Res. Otolaryngol.*, 9:417–435, 2008.

R. Schaette and R. Kempter. Development of tinnitus-related neuronal hyperactivity through homeostatic plasticity after hearing loss: a computational model. *Eur. J. Neurosci.*, 23:3124–3138, 2006.

R. Schaette and R. Kempter. Development of hyperactivity after hearing loss in a computational model of the dorsal cochlear nucleus depends on neuron response type. *Hear. Res.*, 240:57–72, 2008.

Y. Shiomi, J. Tsuji, Y. Naito, N. Fujiki, and N. Yamamoto. Characteristics of DPOAE audiogram in tinnitus patients. *Hear. Res.*, 108:83–88, 1997.

S. K. Suneja, C. G. Benson, and S. J. Potashner. Glycine receptors in adult guinea pig brain stem auditory nuclei: regulation after unilateral cochlear ablation. *Exp. Neurol.*, 154:473–488, 1998a.

S. K. Suneja, S. J. Potashner, and C. G. Benson. Plastic changes in glycine and GABA release and uptake in adult brain stem auditory nuclei after unilateral middle ear ossicle removal and cochlear ablation. *Exp. Neurol.*, 151: 273–288, 1998b.

G. G. Turrigiano. Homeostatic plasticity in neuronal networks: the more things change, the more they stay the same. *Trends Neurosci.*, 22:221–227, 1999.

G. G. Turrigiano, K. R. Leslie, N. S. Desai, L. C. Rutherford, and S. B. Nelson. Activity-dependent scaling of quantal amplitude in neocortical neurons. *Nature*, 391:892–896, 1998.

T. Tzounopoulos, Y. Kim, D. Oertel, and L. O. Trussell. Cell-specific, spike timing-dependent plasticities in the dorsal cochlear nucleus. *Nat. Neurosci.*, 7:719–725, 2004.

C. Vale and D. H. Sanes. The effect of bilateral deafness on excitatory and inhibitory synaptic strength in the inferior colliculus. *Eur. J. Neurosci.*, 16:2394–2404, 2002.

N. Weisz, T. Hartmann, K. Dohrmann, W. Schlee, and A. Norena. High-frequency tinnitus without hearing loss does not mean absence of deafferentation. *Hear. Res.*, 222:108–114, 2006.

E. D. Young and K. A. Davis. Circuitry and function of the dorsal cochlear nucleus. In D. Oertel, R. R. Fay, and A. N. Popper, editors, *Integrative Functions in the Mammalian Auditory Pathway*, volume 15 of *Springer Handbook of Auditory Research*, chapter 5, pages 121–157. Springer, New York, 2002.

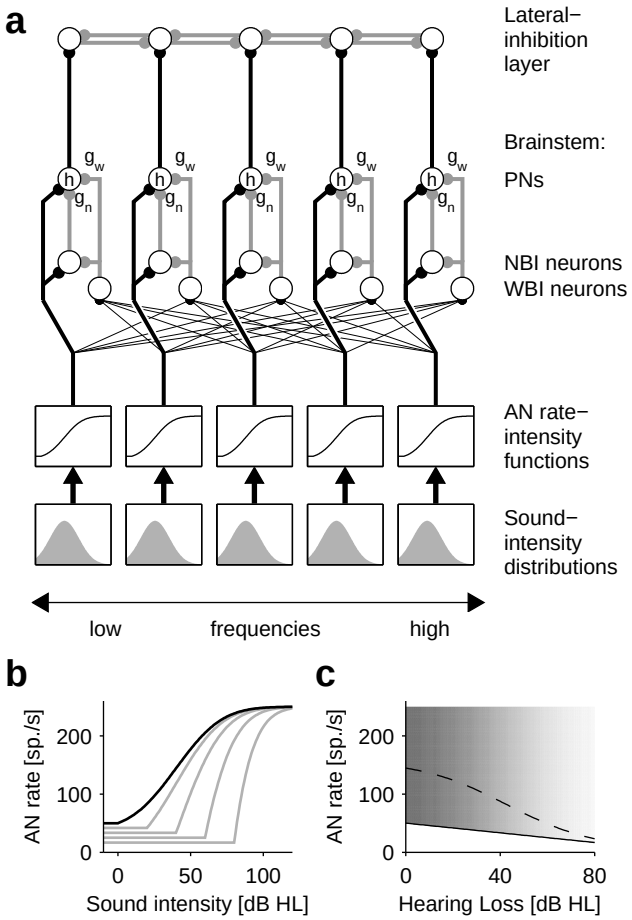

Figure 1: Model architecture. **a)** Neurons (large circles), excitatory connections (black lines), and inhibitory connections (gray lines). Frequency channels are tonotopically arranged; 5 channels are shown. In each frequency channel, the acoustic environment is described by a Gaussian distribution of sound intensity, which is transformed to auditory nerve (AN) activity by a rate-intensity function. The brainstem stage of the model consists of projection neurons (PNs) and inhibitory interneurons (wide-band inhibitor: WBI, narrow-band inhibitor: NBI). The strength of the inhibitory projections onto the PNs is regulated by the gain factors g_{w} and g_{n}. The mean firing rates of the PNs are stabilized by homeostatic plasticity (homeostasis factor h). The highest stage of the model is a layer of neurons with lateral inhibitory connections. **b)** In a rate-intensity model of AN activity, the effects of noise-induced hearing loss on AN activity are captured by increasing the response threshold and decreasing the spontaneous firing rate (black line: healthy, gray lines: hearing loss). **c)** Distribution of AN firing rates as a function of hearing loss. The mean firing rate of the AN fiber population (dashed line) is decreased in proportion to the severity of hearing loss. The solid line denotes the spontaneous firing rate, and the shaded area indicates the distributions of firing rates, where the gray level stands for the probability of occurrence of a specific firing rate.

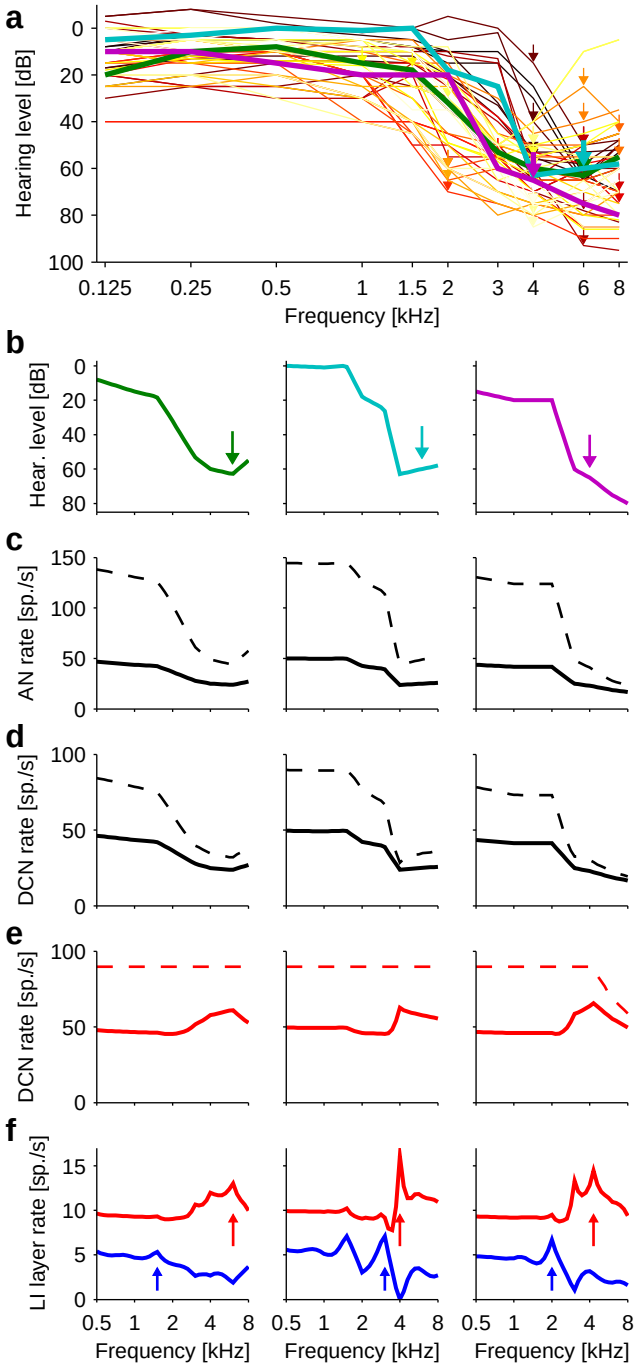

Figure 2: Estimation of tinnitus pitch from audiograms. **a)** Audiograms (colored lines) and tinnitus pitch matching results (downward arrows) of 24 subjects with noise-induced hearing loss and tone-like tinnitus. **b)** Audiograms of three subjects with tinnitus pitch (downward arrows) of 6 kHz, 6 kHz, and 4 kHz. **c)** Firing rate of the model AN adjusted to each subject's hearing loss. In each case, mean (dashed lines) and spontaneous (solid lines) firing rates are decreased in the high-frequency range. **d)** Same as (c), but for PNs of the DCN before homeostasis. **e)** Same as (d), but after homeostasis. **f)** Lateral-inhibition-layer neurons. Red lines: when driven by the patterns of spontaneous firing rates of DCN PNs after homeostasis (shown in e), the activity of the neurons peaks at frequencies (red upward arrows) that are close to the patients' tinnitus pitch. Blue lines: when driven by the spontaneous activity of DCN neurons before or without homeostasis (shown in d), activity of the neurons has peaks at frequencies (blue upward arrows) close to the audiogram edge.

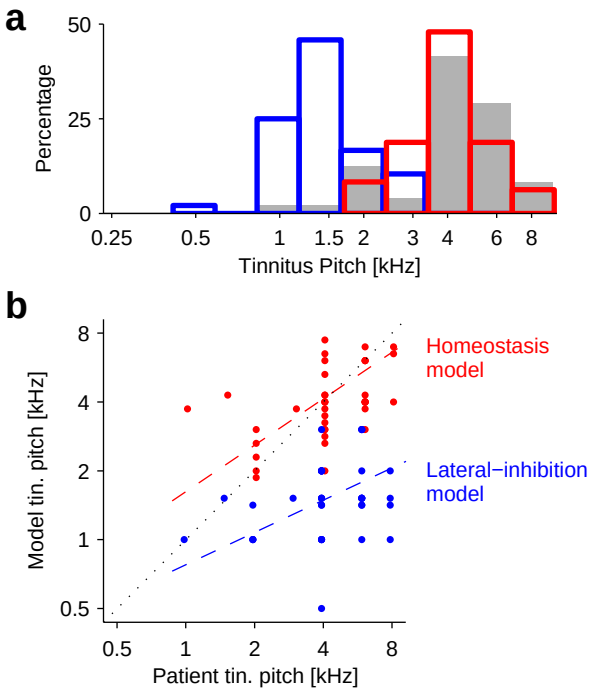

Figure 3: Homeostasis model vs. lateral-inhibition model. **a)** Distributions of tinnitus pitch: measured (gray bars) and estimated from the homeostasis model (bars with red outlines) and the lateral-inhibition model (bars with blue outlines). **b)** Scatter plots of estimated versus observed tinnitus pitch (red dots: full model with homeostasis; blue dots: lateral-inhibition model; dashed lines: regression lines; dotted line: identity). Note that colored dots may lie on top of each other. The predictions of the homeostasis model are almost unbiased ($B = -0.05$ octaves) with a low prediction error ($E = 0.60$ octaves) and a high correlation coefficient ($C = 0.49$). The lateral-inhibition model predicts tinnitus pitch systematically too low ($B = -1.47$ octaves) with a high prediction error ($E = 1.62$ octaves) and a low correlation coefficient ($C = 0.37$). Model parameters: $g_{\mathrm{n}} = 1.3$, $g_{\mathrm{w}} = 0.6$, $h_{\max} = 3$.

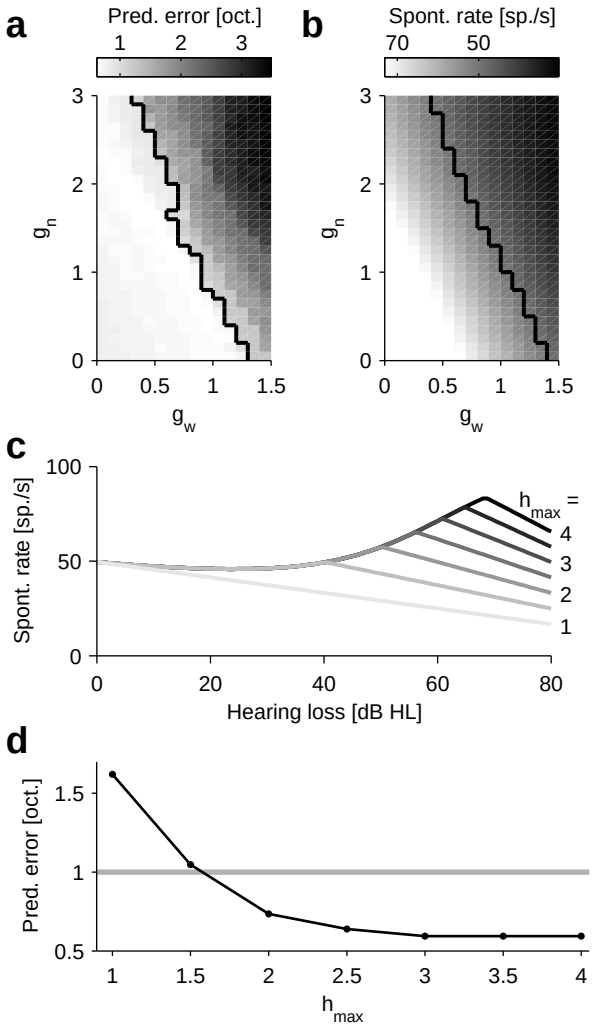

Figure 4: Dependence of pitch prediction performance on model parameters. **a)** Pitch prediction error E (gray-scale coded) of the homeostasis model for different values of the inhibitory gain factors g_{w} and g_{n} ($h_{\max} = 3$); black contour line indicates $E = 1$ octave. **b)** Spontaneous firing rates (gray-scale coded) of PNs after 60 dB noise-induced hearing loss and homeostatic plasticity ($h_{\max} = 3$). **c)** Spontaneous firing rates of DCN PNs ($g_{\mathrm{w}} = g_{\mathrm{n}} = 0.5$) after homeostasis for different degrees of hearing loss and different values of $h_{\max}$ from 1 to 4 in steps of 0.5 ($h_{\max} = 1$: homeostasis disabled). **d)** Pitch prediction error (minimum in the g_{w}-g_{n} plane as in (a)) as a function of $h_{\max}$.

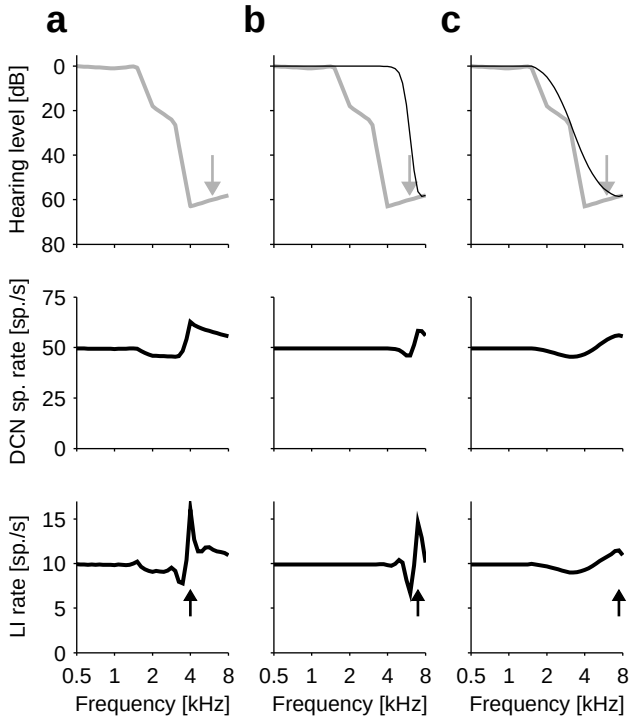

Figure 5: Impact of hearing aids on spontaneous-activity profiles. Top row: audiogram (gray lines), tinnitus pitch (arrows), and effective audiograms (black lines in b and c) that include a hearing aid. Center row: spontaneous firing rates of model DCN PNs after homeostasis. Bottom row: spontaneous firing rates in the lateral-inhibition layer. **a)** Without a hearing aid, spontaneous firing rates are increased in the high-frequency region of the model DCN, leading to a pronounced tinnitus peak at 4 kHz in the lateral-inhibition layer (same as in the middle column of Figs. 2b, e and f). **b)** A hypothetical perfect hearing aid that completely normalizes AN activity up to an upper cut-off frequency of 6 kHz leads to an effective audiogram (top panel, black line) with an audiogram edge at a higher frequency and a steep slope. The resulting spontaneous firing rates of DCN PNs are normal up to about 6 kHz, but elevated at higher frequencies. There and in the activity profile of the lateral-inhibition layer, we recognize a peak at 7 kHz. **c)** Stimulation with a hearing aid adjusted to create an effective audiogram with a smooth edge and a shallow slope (top panel, black line) leads to broad and smooth profiles of spontaneous firing rates without pronounced peaks in the model DCN and lateral-inhibition layer.